Environ. Sci. Technol. **2005**, *39,* 4441−4446

Isoprene Forms Secondary Organic Aerosol through Cloud Processing: Model Simulations

HO-JIN LIM,[†]
ANNMARIE G. CARLTON, AND
BARBARA J. TURPIN*

Department of Environmental Sciences, Rutgers University, 14 College Farm Road, New Brunswick, New Jersey 08901

Isoprene accounts for more than half of non-methane volatile organics globally. Despite extensive experimentation, homogeneous formation of secondary organic aerosol (SOA) from isoprene remains unproven. Herein, an in-cloud process is identified in which isoprene produces SOA. Interstitial oxidation of isoprene produces water-soluble aldehydes that react in cloud droplets to form organic acids. Upon cloud evaporation new organic particulate matter is formed. Cloud processing of isoprene contributes at least 1.6 Tg yr^{-1} to a global biogenic SOA production of 8−40 Tg yr^{-1}. We conclude that cloud processing of isoprene is an important contributor to SOA production, altering the global distribution of hygroscopic organic aerosol and cloud condensation nuclei.

Introduction

Organic particulate matter (PM) accounts for 20−70% of fine aerosol mass. The role of organic PM in regional and global climate change has received much recent attention (*1*−*4*). Organic PM affects radiative forcing directly through scattering and indirectly by changing cloud microphysics. It is predicted to have a net cooling effect on global climate forcing (*1*). However, there are large uncertainties in current forcing estimates. Organic PM consists of primary organic aerosol (POA) emitted directly into the atmosphere and secondary orgainc aerosol (SOA) formed in the atmosphere from reactive organic gases. The relative abundance of POA and SOA contributes to forcing estimate uncertainties because SOA is more polar and hygroscopic than POA (*4*). Hygroscopic SOA could provide cloud condensation nuclei (CCN) and therefore play an important role in microphysical cloud processes (*5*, *6*). Although the contribution of SOA to organic aerosols is certainly substantial (*1*), formation mechanisms and precursors require further elucidation (*4*).

SOA formation from condensation/sorption of low-volatility products of gas-phase photochemical reactions is well documented. However, isoprene has not been shown to contribute to SOA formation through this mechanism, despite numerous experiments to investigate the homogeneous oxidation of isoprene. It was suggested that particulate 2-methyltetrols found in the Amazon are formed through the homogeneous oxidation of isoprene (*7*). However, in a subsequent paper these authors concluded that the atmospheric dynamics of 2-methyltetrols and related species was not consistent with a homogeneous mechanism and was instead consistent with formation in the aqueous aerosol phase by acid-catalyzed reaction with hydrogen peroxide (*8*). Enhanced SOA formation through acid-catalyzed reactions on particle surfaces has recently been convincingly demonstrated (*9*) and provides a proven mechanism by which isoprene can yield SOA (*10*, *11*). In addition, fog/cloud processing, which is an important source of sulfate, has been hypothesized to be an important source of SOA (*12*). Compelling recent evidence supports this hypothesis (*13*−*15*). Briefly, reactive organics are oxidized in the interstitial spaces to form highly water-soluble compounds (e.g., aldehydes) that readily partition into cloud droplets. (OH concentrations are elevated in the interstitial spaces of clouds (*16*).) The dissolved organics oxidize further to form less volatile organics, e.g., organic acids. Upon cloud droplet evaporation, these organics remain in the particle phase and add to the budget of hygroscopic SOA. In this study we demonstrate that isoprene forms hygroscopic SOA through cloud processing.

Water-soluble organic diacids (C2−C10) contribute as much as 1−3% and 10% of urban and remote marine particulate carbon, respectively (*17*). Diurnal and seasonal variations suggest that they are predominantly of secondary, photochemical origin (*18*−*20*), but their formation is not well understood. In-cloud oxalic acid concentrations (0.21 $\mu g\,m^{-3}$) were 3 times greater than below-cloud concentrations off the coast of California (*13*). In that study and elsewhere oxalic acid tends to be found in the droplet rather than condensation mode (*13*, *17*, *21*). Both observations are consistent with an aqueous-phase formation mechanism since the droplet mode forms when new particulate material is added to condensation mode particles through aqueous-phase reactions (*22*).

Glyoxal and glyoxylic acid are recognized as potential precursors of oxalic acid on the basis of their concentration dynamics (*18*, *20*). However, gas-phase oxidation and photolysis of these compounds are unlikely to produce oxalic acid (*23*). A recent cloud chemistry model predicts substantial oxalic acid formation through α-dicarbonyl intermediates from ethylene and acetylene (*14*). Reactions of the dissolved carbonyls with OH in cloud droplets produce glyoxylic acid, pyruvic acid, and oxalic acid (*24*, *25*). Interestingly, these water-soluble carbonyls have a direct link to isoprene, which has a global annual emission of ∼500 Tg, comparable to the natural global emissions of methane (*26*). Isoprene is omnipresent in the troposphere at a mixing ratio of about 0.1−7 ppb by season and location (*27*). Gas-phase oxidation of isoprene shows high yields of the water-soluble carbonyls (*28*, *29*). Its high emission, concentration, reactivity, and yield of water-soluble carbonyls well qualify isoprene to be an important precursor of SOA formation through cloud processing. Although the large influence of isoprene on tropospheric ozone is well understood, its contribution to SOA was believed to be negligible (*30*) until very recently when heterogeneous pathways began to be investigated. If isoprene produces organic acids through cloud chemistry, its contribution to regional and global SOA warrants reconsideration.

Methods

We developed a photochemical box model to investigate SOA formation through cloud processing of isoprene. The box model assumes monodisperse cloud droplets, homogeneously mixed species within the interstitial space and within

* Corresponding author phone: (732)932-9540; fax: (732)932-8644; e-mail: turpin@aesop.rutgers.edu.

[†] Present address: Department of Environmental Engineering, Kyungpook National University, 1370 Sankyuk-dong, Buk-gu, Daegu 702-701, Korea.

10.1021/es048039h CCC: $30.25
Published on Web 05/12/2005

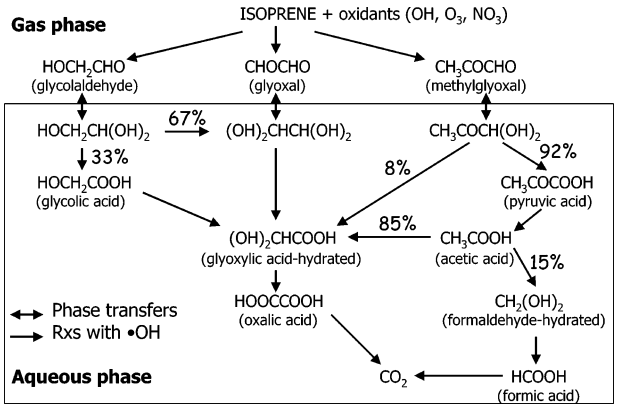

FIGURE 1. In-cloud isoprene chemistry for the formation of hygroscopic organic acids: glycolic acid, glyoxylic acid, pyruvic acid, and oxalic acid.

the cloud droplets, no temporal evolution of physical cloud properties, and constant temperature and pressure. The mass balance of a species in the gas and aqueous phase depends on chemical reactions, phase transfers between the gas and aqueous phases, emissions, and dry deposition. It neglects aerosol deposition.

The chemical mechanism in the model is based on previous cloud chemistry mechanisms (*14*, *31*) and a condensed version of isoprene chemistry for RADM2 (*29*, *32*). Chemical reactions involving water-soluble carbonyl products of isoprene were added. Figure 1 shows the proposed pathway for in-cloud isoprene oxidation. Briefly, gas-phase isoprene oxidation produces glycolaldehyde, glyoxal, and methylglyoxal. These products dissolve into water and react with OH radical to form oxalic acid via glycolic acid, glyoxylic acid, pyruvic acid, and acetic acid. The aqueous-phase chemical mechanism is very similar to another recent cloud photochemistry model (*15*) except for the fate of methylglyoxal. In the previous model the reaction between methylglyoxal and OH yields pyruvic acid, which is further oxidized to acetaldehyde and finally CO_2 without forming low-volatility organic acids. In the current model, methylglyoxal oxidation yields pyruvic acid, acetic acid, glyoxylic acid, and finally oxalic acid. This pathway reproduces well the kinetics of methylglyoxal oxidation in studies of acetone degradation by H_2O_2/UV (*25*). Detailed chemical analyses show good closure in the carbon mass of the proposed degradation mechanism. The previous model underestimates the role of isoprene in organic acid formation.

The mass balance of a species in the gas and aqueous phases depends on chemical reactions, emissions, and dry deposition as shown in eqs 1 and 2,

$$\frac{dC_g}{dt} = Q_g - S_g + \frac{J_e}{Z_{bl}} - \frac{v_d C_g}{Z_{bl}} - Lk_t C_g + \frac{k_t C_a}{H_{eff} RT} \quad (1)$$

$$\frac{dC_a}{dt} = Q_a - S_a + Lk_t C_g - \frac{k_t C_a}{H_{eff} RT} \quad (2)$$

respectively, where C_g = gas-phase concentration (molecules cm^{-3}), C_a = aqueous-phase concentration (mol^{-1} L^{-1}), Q_g = gas-phase source reactions (molecule cm^{-3} s^{-1}), Q_a = aqueous-phase source reactions (mol L^{-1} s^{-1}), S_g = gas-phase sink reactions (molecule cm^{-3} s^{-1}), S_a = aqueous-phase sink reaction rates (mol L^{-1} s^{-1}), J_e = emission flux (molecules cm^{-1} s^{-1}), Z_{bl} = height of the boundary layer (cm), v_d = dry deposition velocity (cm s^{-1}), L = liquid water content (g m^{-3}), k_t = phase-transfer coefficient (s^{-1}), H_{eff} = effective Henry's constant (mol L^{-1} atm^{-1}), R = ideal gas constant (atm L mol^{-1} K^{-1}), and T = temperature (K). Equation 3 describes the

$$k_t = \left(\frac{a^2}{3D_g} + \frac{4a}{3v\alpha}\right)^{-1} \quad (3)$$

coefficient used to compute phase transfer between the gas and aqueous phases (*33*), where a = droplet radius (cm), D_g = gas-phase diffusivity (cm^2 s^{-1}), v = mean molecular speed (cm s^{-1}), and α = accommodation coefficient (dimensionless). The gas-phase diffusivity and mean molecular speed were calculated using eqs 4 (*34*) and 5 (*35*),

$$D_g = 1.9(MW)^{-2/3} \quad (4)$$

$$v = \left(\frac{8k_b TN_a}{\pi(MW)}\right)^{1/2} \quad (5)$$

respectively, where MW = molecular weight (g mol^{-1}), k_b = Boltzmann constant (1.38×10^{-16} dyn cm K^{-1}), T = temperature (K), and N_a = Avogadro's number (6.023×10^{23} molecules mol^{-1}). Numerical solutions of the mass balance were obtained using FACSIMILE (*36*).

The modeled chemical mechanism is provided in the Supporting Information and includes gas- and aqueous-phase chemical species, equatorial summertime photolysis frequencies, thermal reactions, aqueous-phase equilibrium, Henry's law constants, accommodation coefficients for water-soluble species, emission fluxes, and dry deposition velocities. Initial concentrations of species for the base run (P00) are also provided in the Supporting Information. Formaldehyde (MVKP) is one of the main intermediate products of isoprene chemistry (*37*). In other models carbonyl products of the reaction of MVKP and NO are represented as ALD (aldehydes with ≥2 carbons). In this model ALD was changed to glycolaldehyde (GCOL) as below:

$$MVKP + NO \rightarrow 0.7CH_3CO_3 + 0.8GCOL + 0.3CH_2O + 0.3HO_2 + 0.3MGLY + NO_2$$

where MGLY is methylglyoxal. This was done because glycolaldehyde is a dominant contributor to ALD (*38*, *38*), and other aldehydes represented as ALD are likely very similar to glycolaldehyde in chemical properties such as water solubility and reactivity. This modification was important to the purpose of this paper since the water solubility of the products is critical to assessing the importance of isoprene on secondary organic aerosol formation through cloud processing.

We simulated cloud processing of isoprene in an air parcel as it was transported for 5 days over the tropical Amazon followed by 5 days over the Atlantic Ocean. The Amazon is a major source (13% of global emissions) of isoprene (*40*). Photolysis occurred semisinusoidally between 0600 and 1800 hours local time with a peak at noon and no nighttime photolysis. Clouds were present daily between 1300 and 1600 hours. The base run (P00) assumed 10 μm diameter cloud droplets and a liquid water content of 0.5 g m^{-3}. The cloud temperature and altitude were 285 K and 1.0 km. The relative humidity was kept constant at 100% and 75% during the cloud and cloudless periods, respectively. The simulation began at 0600 hours ($t = 0$) with emission and deposition conditions representative of a remote continental area. These conditions changed to represent a remote marine area at 0600 hours on day 6. Emissions were held constant except for the isoprene flux, which varied semisinusoidally between 0600 and 1800 hours with a peak at noon and no nighttime emission. The peak isoprene emission flux was 1.01×10^{12} molecules cm^{-2} s^{-1}, typical of the tropical Amazon (*41*). It dropped to zero over the remote marine area on days 6−10. Aqueous-phase reactions and phase transfers occurred only during cloud periods. Following each cloud period aqueous-

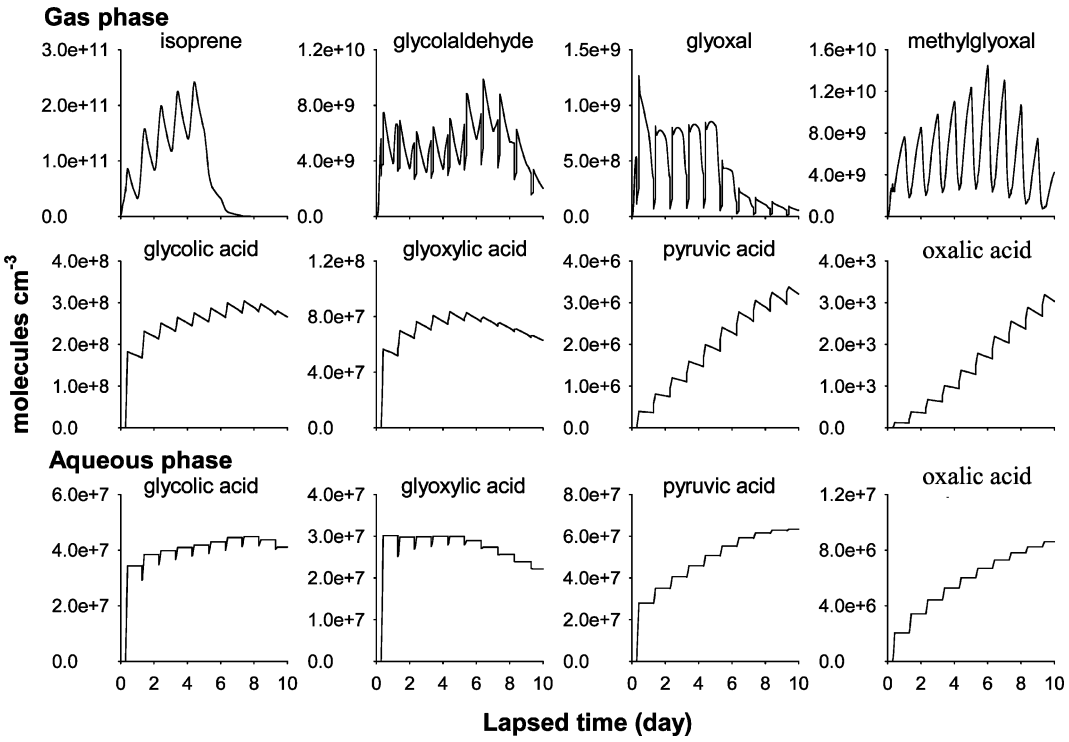

FIGURE 2. Isoprene, glycolaldehyde, glyoxal, and methylglyoxal concentrations (gas-phase) and glycolic acid, glyoxylic acid, pyruvic acid, and oxalic acid concentrations (gas- and aqueous-phase) predicted by base run simulation (P00).

phase species continued evaporating from cloud droplets, while gas-phase species were not allowed to dissolve or react in the droplets. No phase transfer was allowed for the low-volatility organic acids (i.e., glycolic, pyruvic, glyoxylic, and oxalic acid) during the cloudless period.

Results

Figure 2 shows the concentrations of important gas- and aqueous-phase species over the 10-day run. Gas-phase isoprene concentrations exhibited a distinctive diurnal variation over land and dropped rapidly on day 6 when isoprene emissions ended. Isoprene accumulated with time from day 1 to day 5, suggesting that the model underpredicted nighttime removal, similar to previous remote continental predictions (*42*). A large fraction of glycolaldehyde, glyoxal, and methylglyoxal dissolved into cloud droplets during the cloud period and returned to the gas phase after the cloud period. The oxidation of dissolved carbonyls produced glycolic acid, glyoxylic acid, pyruvic acid, and oxalic acid, at concentrations that kept increasing while interstitial isoprene chemistry supplied carbonyl precursors. Aqueous-phase plots in Figure 2 provide the concentration of each organic acid summed over all charge states. Oxalic acid concentrations continued to increase even over the ocean (days 6−10) due to the continued oxidation of precursors.

Figure 3 shows organic acid concentrations in the gas and aqueous phases before the end of each cloud period, and estimated gas and particle concentrations after cloud evaporation. Particulate organic acid concentrations after cloud evaporation were estimated from the total amount of product (gas phase plus aqueous phase) and gas/particle partitioning measurements in the literature. Specifically, 90%, 75%, 75%, and 70% of oxalic acid, glyoxylic acid, glycolic acid, and pyruvic acid, respectively, are expected to remain in the particle phase after cloud droplet evaporation (*43*). After three and eight cloud periods total concentrations of glycolic acid, glyoxylic acid, pyruvic acid, and oxalic acid were 37 and 44, 13 and 12, 6.1 and 9.5, and 0.66 and 1.2 ng m^{-3}, respectively. Particulate oxalic acid concentrations after

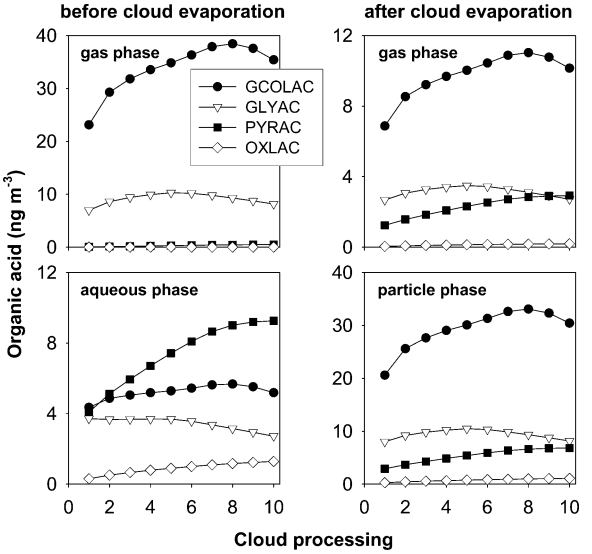

FIGURE 3. Gas- and aqueous-phase concentrations of organic acids formed through cloud processing of isoprene and the corresponding gas- and particulate-phase concentrations after cloud evaporation predicted by base run simulation (P00): glycolic acid (GCOLAC), glyoxylic acid (GLYAC), pyruvic acid (PYRAC), and oxalic acid (OXLAC).

one, three, eight, and ten cloud cycles were 0.26, 0.56, 0.99, and 1.1 ng m^{-3}, respectively. Particulate total organic acid concentrations after one, three, eight, and ten cloud cycles were 32, 42, 50, and 46 ng m^{-3}, respectively. Although this model considered organic acids to be only in the acidic or dissociated form, organic acids can also form less soluble salts of inorganic cations in cloud droplets. The formation of organic salts will result in increased particulate organic acid concentrations beyond model prediction.

Figure 4A shows particulate organic acid concentrations after three cloud processings at different isoprene emissions [(P02) 0, (P03) 0.05, (P04) 0.1, (P05) 0.5, (P06) 1.5, and (P07)

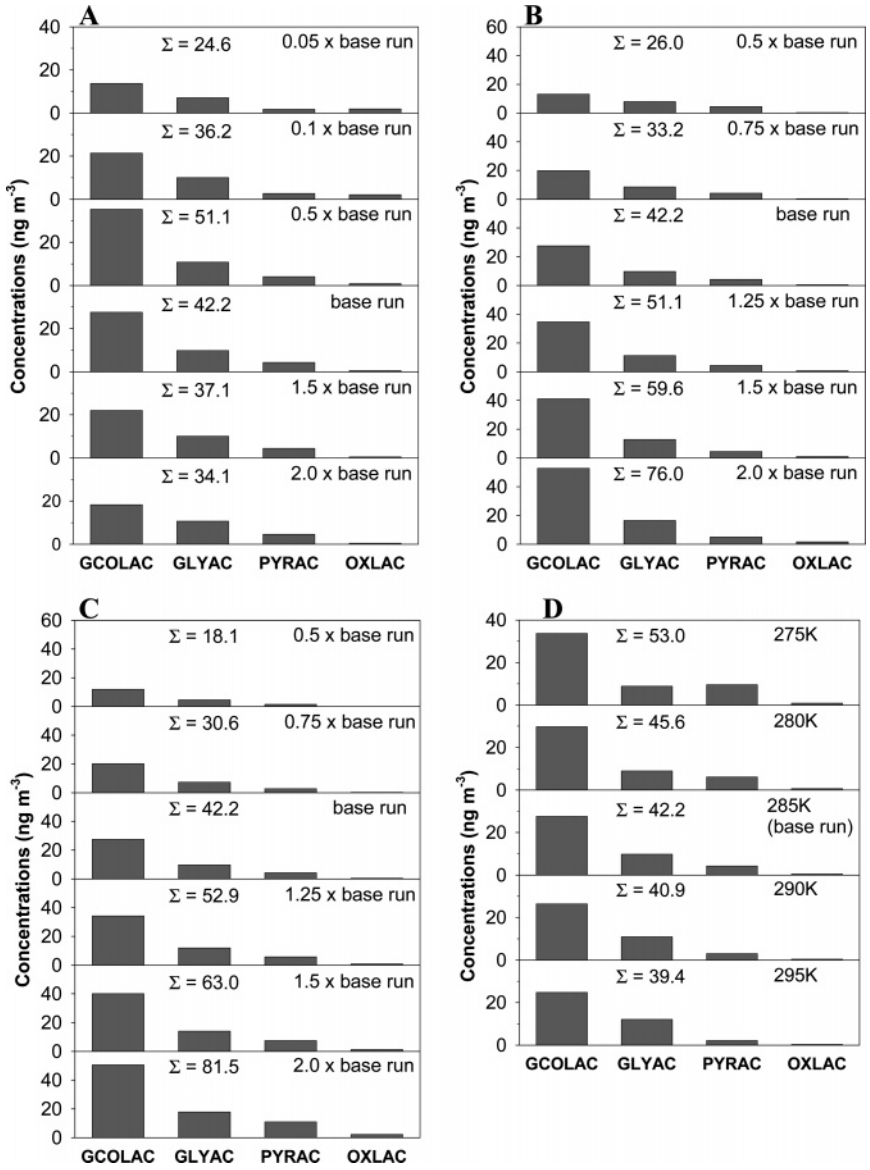

FIGURE 4. Particulate concentrations of glycolic acid (GCOLAC), glyoxylic acid (GLYAC), pyruvic acid (PYRAC), and oxalic acid (OXLAC) after three cloud processings with increasing (A) isoprene emission flux, (B) photolysis frequency, (C) liquid water content, and (D) temperature.

2.0 × base run]. Total concentrations of particulate organic acids for P02, P03, P04, P05, P00, P06, and P07 were 0, 25, 36, 51, 42, 37, and 34 ng m^{-3}, respectively. Gas-phase methylglyoxal concentrations just before the cloud period of day 3 for P02, P03, P04, P05, P00, P06, and P07 were 3.2×10^5, 3.0×10^8, 5.8×10^8, 1.8×10^9, 2.3×10^9, 2.7×10^9, and 3.0×10^9 molecules cm^{-3}, respectively. At the same time OH concentrations in the gas phase for P02, P03, P04, P05, P00, P06, and P07 were 7.8×10^6, 6.5×10^6, 5.1×10^6, 6.6×10^5, 2.6×10^5, 1.6×10^5, and 1.2×10^5 molecules cm^{-3}, respectively. During the cloud period of day 3 aqueous-phase OH concentrations for P02, P03, P04, P05, P00, P06, and P07 were 7.2, 4.2, 2.9, 0.90, 0.83, 0.83, and 0.81 molecules cm^{-3}, respectively. An increase in the isoprene emissions resulted in increased α-carbonyl concentrations due to the high reactivity of isoprene and also decreased OH concentrations. The high reactivity of isoprene with OH accounts for 71% of OH removal in the Amazon (*40*). Daytime OH concentrations of 2.3×10^5 molecules cm^{-3} at day 5 for the base run were about 30 times lower than 6.3×10^6 molecules cm^{-3} at day 5 for P04 (isoprene emission = 0.1 × base run). Thus, aqueous-phase reactions at higher isoprene emissions were OH limited, resulting in the nonlinear trend of organic acid concentrations shown in Figure 4A. Decreased OH concentrations at high isoprene emissions have been predicted previously for remote conditions (*42*).

Photolysis is not only a main source of OH radicals but also an effective destruction pathway for carbonyl precursors. Figure 4B shows organic acid formation at various photolysis rates [(P09) 0.5, (P10) 0.75, (P11) 1.25, (P12) 1.5, and (P13) 2.0 × base run]. Increasing photolysis rates from P09 to P10, P00, P11, P12, and P13 resulted in the increased organic acid concentrations from 26 to 33, 42, 51, 60, and 76 ng m^{-3}, respectively. Gas-phase concentrations of OH, HO_2, and H_2O_2 also increased with increasing photolysis. Hydroxyl radial concentrations for P09, P00, and P13 were 1.3×10^5, 2.5×10^5, and 5.9×10^5 molecules cm^{-3}, respectively. Gas-phase glyoxal and methylglyoxal concentrations decreased substantially with the increased photolysis [glyoxal, methylglyoxal: (P09) 5.7×10^8, 4.4×10^9, (P00) 3.5×10^8, 2.3×10^9, and (P13) 2.1×10^8, 1.3×10^9 molecules cm^{-3}], although glycolaldehyde concentrations increased somewhat with increasing photolysis rates [(P09) 4.7×10^9, (P00) 5.3×10^9, and (P13) 5.8×10^9 molecules cm^{-3}]. Again, this demonstrates that the availability of aqueous-phase OH is critical for organic acid formation.

Figure 4C shows the influence of liquid water content on cloud processing [(P09) 0.5, (P10) 0.75, and (P11) 1.25 × base run). Organic acid concentrations increased linearly as a function of liquid water content in the range between 0.25 and 1.0 g m^{-3}. Interstitial isoprene oxidation is likely a large enough pool of water-soluble aldehydes and OH radicals for organic acid formation in cloud droplets. Interestingly, lower temperatures favored organic acid formation (see Figure 4D) due to the temperature dependence of water solubility and reaction kinetics. In cold regions this temperature effect can compensate for the lower photochemical activity. The sensitivity analyses for temperature did not include the effect of temperature on gas/particle partitioning. Lower temperatures also increase partitioning of products to the particle phase.

Discussion and Implications

This study demonstrates the substantial production of hygroscopic organic acids through the cloud processing of isoprene under realistic tropical conditions. About 50 ng m^{-3} organic acids including ~1 ng m^{-3} oxalic acid were predicted to form with an isoprene emission typical of the Amazon. For several reasons stated above, this estimate is likely to be a lower bound. Oxalic acid measurements in the remote and marine atmosphere range from 10 to 50 and from 9 to 693 ng m^{-3}, respectively (*14*, *44*). Sensitivity analyses suggest that the cloud processing of isoprene is omnipresent and ubiquitous. The isoprene emission rate is unlikely to be the most critical factor affecting the overall yield of organic acids; however, it affects the composition of organic acids. The most oxidized product, oxalic acid, tends to increase both in absolute and fractional amounts at lower isoprene emissions. Organic acid production (and partitioning to the particle phase) increases at lower temperatures. Therefore, organic acid formation by cloud processing is likely to be important in various regions with an isoprene emission between 5.0×10^{10} and 1.0×10^{12} molecules cm^{-2} s^{-1} and temperature between 275 and 295 K.

The contribution of cloud processing to the global SOA budget appears to be considerable. After three cloud processings particulate oxalic acid and total particulate organic acid concentrations were estimated to be 0.56 and 42 ng m^{-3} (3.75×10^6 and 3.31×10^8 molecules cm^{-3}), respectively. The predicted concentrations correspond to 0.0033% and 0.29% in volume (0.0043% and 0.33% in mass) of an isoprene mixing ratio of 5 ppb (1.14×10^{11} molecules cm^{-3}) (*7*). By taking into account the apparent yields, a global isoprene emission flux of 500 Tg yr^{-1} results in an SOA source strength from cloud processing of 1.6 Tg yr^{-1} (0.022 Tg yr^{-1} of oxalic acid). This is a substantial contribution to global biogenic SOA (8−40 Tg yr^{-1}) (*1*).

The cloud processing of isoprene forms hygroscopic SOA that can serve as CCN and influence regional and global climate change. SOA formation by cloud processing is also predicted to be important in polluted regions, because anthropogenic pollutants including aromatics are a substantial source of water-soluble aldehydes and ketones (*15*, *32*). The possibility of SOA formation through aqueous-phase isoprene chemistry on deliquesced particles in clear sky also warrants further examination. One limitation of the current model is that it does not allow for phase transfer of low-volatility organic acids. Evaporation and gas-phase reaction of pyruvic acid (*45*) could reduce SOA formation. On the other hand, formation of organic salts will increase SOA formation. Also, it would not be surprising if aldehydes and organic acids (including pyruvic acid) form oligomers in cloudwater, increasing SOA formation (*9*, *46*−*48*). Formation of other SOA products through cloud processing, such as polyols, is also possible.

Acknowledgments

This research has been supported by a grant from the U.S. Environmental Protection Agency's Science to Achieve Results (STAR) program (Grant R831073). Although the research described in this paper has been funded wholly or in part by the U.S. Environmental Protection Agency's STAR program, it has not been subjected to any EPA review and therefore does not necessarily reflect the views of the Agency, and no official endorsement should be inferred.

Supporting Information Available

Modeling mechanism (Tables S1−S11). This material is available free of charge via the Internet at http://pubs.acs.org.

Literature Cited

(1) Intergovernmental Panel on Climate Change (IPCC). *Climate Change 1994*; Cambridge University Press: New York, 1995.

(2) Novakov, T.; Penner, J. E. Large contribution of organic aerosols to cloud-condensation-nuclei concentrations. *Nature* **1993**, *365*, 823−826.

(3) Ramanathan, V.; Crutzen, P. J.; Kiehl, J. T.; Rosenfeld, D. Aerosols, climate, and hydrological cycle. *Science* **2001**, *294*, 2119−2124.

(4) Kanakidou, M.; Sienfeld, J. H.; Pandis, S. N.; Barnes, I.; Dentener, F. J.; Facchini, M. C.; van Dingenen, R.; Ervens, B.; Nenes, A.; Nielsen, C. J.; Swietlicki, E.; Putaud, J. P.; Balkanski, Y.; Fuzzi, S.; Horth, J.; Moortgat, G. K.; Winterhalter, R.; Myhre, C. E. L.; Tsigaridis, K.; Vignati, E.; Stephanou, E. G.; Wilson, J. Organic aerosol and global climate modeling: A review. *Atmos. Chem. Phys. Discuss.* **2004**, *4*, 5855−6024.

(5) Cruz, C. N.; Pandis, S. N. A study of the ability of pure secondary organic aerosol to act as cloud condensation nuclei. *Atmos. Environ.* **1997**, *31*, 2205−2214.

(6) Peng, C.; Chan, C. K. The water cycle of water-soluble organic salts of atmospheric importance. *Atmos. Environ.* **2001**, *35*, 1183−1192.

(7) Claeys, M.; Graham, B.; Vas, G.; Wang, W.; Vermeylen, R.; Pashynska, V.; Cafmeyer, J.; Guyon, P.; Andreae, M. O.; Artaxo, P.; Maenhaut, W. Formation of secondary organic aerosols through photooxidation of isoprene. *Science* **2004**, *303*, 1173−1176.

(8) Claeys, M.; Wang, W.; Ion, A. C.; Kourtchev, I.; Gelencser, A.; Maenhaut, W. Formation of secondary organic aerosols from isoprene and its gas-phase oxidation products through reaction with hydrogen peroxide. *Atmos. Environ.* **2004**, *38*, 4093−4098.

(9) Jang, M. S.; Czoschke, N. M.; Lee, S.; Kamens, R. M. Heterogeneous atmospheric aerosol production by acid-catalyzed particle-phase reactions. *Science* **2002**, *298*, 814−817.

(10) Czoschke, N. M.; Jang, M.; Kamens, R. M. Effect of acidic seed on biogenic secondary organic aerosol growth. *Atmos. Environ.* **2003**, *37*, 4287−4299.

(11) Limbeck A.; Kulmala M.; Puxbaum H. Secondary organic aerosol formation in the atmosphere via heterogeneous reaction of gaseous isoprene on acidic particles. *Geophys. Res. Lett.* **2003**, *30*, doi:10.1029/2003GL017738.

(12) Blando, J. D.; Turpin, B. J. Secondary organic aerosol formation in cloud and fog droplets: A literature evaluation of plausibility. *Atmos. Environ.* **2000**, *34*, 1623−1632.

(13) Crahan, K. K.; Hegg, D.; Covert, D. S.; Jonsson, H. An exploration of aqueous oxalic production in the coastal marine atmosphere. *Atmos. Environ.* **2004**, *38*, 3757−3764.

(14) Warneck, P. In-cloud chemistry opens pathway to the formation of oxalic acid in the marine atmosphere. *Atmos. Environ.* **2003**, *37*, 2423−2427.

(15) Ervens, B.; Feingold, G.; Frost, G. J.; Kreidenweis, S. M. A modeling study of aqueous production of dicarboxylic acids: 1. Chemical pathways and speciated organic mass production. *J. Geophys. Res.* **2004**, *109*, D15205, doi:10.1029/2003JD004387.

(16) Mauldin, R. L., III; Madronich, S.; Flocke, S. J.; Eisele, F. L.; Frost, G. J.; Prevot, A. S. H. New insights on OH: Measurements around and in clouds. *Geophys. Res. Lett.* **1997**, *24*, 3033−3036.

(17) Kerminen V. M.; Ojanen, C.; Pakkanen, T.; Hillamo, T.; Aurela, R.; Meriläinen, M. Low-molecular weight dicarboxylic acids in an urban and rural atmosphere. *J. Aerosol Sci.* **2000**, *31*, 349−362.18.

(18) Kawamura, K.; Kaplan, I. R. Motor exhaust emission as a primary source of dicarboxylic acids in Los Angeles ambient air. *Environ. Sci. Technol.* **1987**, *21*, 105−110.

(19) Kawamura, K.; Ikushima, K. Seasonal change in the distribution of dicarboxylic acids in the urban atmosphere. *Environ. Sci. Technol.* **1993**, *27*, 2227−2235.
(20) Chebbi, A.; Carlier, P. Carboxylic acids in the troposphere, occurrence, source, and sinks: A review. *Atmos. Environ.* **1996**, *24*, 4233−4249.
(21) Yao, X.; Fang, M.; Chan, C. K. Size distribution and formation of dicarboxylic acids in atmospheric particles. *Atmos. Environ.* **2002**, *36*, 2099−2107.
(22) Meng, Z.; Seinfeld, J. H. On the source of the submicrometer droplet mode of urban and regional aerosols. *Aerosol Sci. Technol.* **1994**, *20*, 253−265.
(23) Koch, S.; Moortgat, G. K. Photochemistry of methylglyoxal in the vapor phase. *J. Phys. Chem.* **1998**, *102*, 9142−9153.
(24) Leitner, N. K. V.; Dore, M. Mechanism of the reaction between hydroxyl radicals and glycolic, glyoxylic, acetic and oxalic acids in aqueous solution: Consequence on hydrogen peroxide consumption in the H_2O_2/UV and O_3/H_2O_2 systems. *Water Res.* **1997**, *31*, 1383−1397.
(25) Stefan, M. I.; Bolton, J. R. Reinvestigation of the acetone degradation mechanism in dilute aqueous solution by the UV/H_2O_2 process. *Environ. Sci. Technol.* **1999**, *33*, 870−873.
(26) Guenther, A.; Hewitt, C. N.; Erickson, D.; Fall, R.; Geron, C.; Graedel, T. E.; Harley, P.; Klinger, L.; Lerdau, M.; McKay, W. A.; Pierce, T.; Scholes, B.; Steinbrecher, R.; Tallamraju, R.; Taylor, J.; Zimmerman, P. A global model of natural volatile organic compound emissions. *J. Geophys. Res.* **1995**, *100*, 8873−8892.
(27) Kuhlmann, R. V.; Lawrence, M. G..; Pöschl, U.; Crutzen, P. J. Sensitivities in global scale modeling of isoprene. *Atmos. Chem. Phys.* **2004**, *4*, 1−17.
(28) Seinfeld, J. H.; Pandis, S. N. *Atmospheric Chemistry and Physics from Air Pollution to Climate Change*; Wiley: New York, 1998; pp 234−336.
(29) Zimmermann, J.; Poppe, D. A supplement for the RADM2 chemical mechanism: The photooxidation of isoprene. *Atmos. Environ.* **1996**, *30*, 1255−1269.
(30) Pandis, S. N.; Paulson, S. E.; Seinfeld, J. H. Aerosol formation in the photooxidation of isoprene and β-pinene. *Atmos. Environ.* **1991**, *25A*, 997−1008.
(31) Warneck, P. The relative importance of various pathways for the oxidation of sulfur dioxide and nitrogen dioxide in sunlit continental fair weather clouds. *Phys. Chem. Chem. Phys.* **1999**, *1*, 5471−5483.
(32) Stockwell, W. R.; Middleton, P.; Chang, J. S.; Tang, X. The second generation regional acid deposition model chemical mechanism for regional air quality modeling. *J. Geophys. Res.* **1990**, *95*, 16343−16367.
(33) Schwartz, S. E. Mass-transport considerations pertinent to aqueous phase reactions of gases in liquid-water clouds. In *Chemistry of Multiphase Atmospheric Systems*; Jaeschke, W., Ed.; Springer-Verlag: Berlin, 1986; pp 415−471.
(34) Schnoor, J. *Environmental Modeling Fate and Transport of Pollutants in Water, Air, and Soil*; Wiley: New York, 1996; pp 327−336.
(35) Lelieveld, J.; Crutzen, P. J. The role of clouds in tropospheric photochemistry. *J. Atmos. Chem.* **1991**, *12*, 229−267.
(36) AEA Technology. *FACSIMILE v4.0 User Guide*; AEA Technology: Oxfordshire, U.K., 2003.
(37) Zimmermann, J.; Poppe, D. A supplement for the RADM2 chemical mechanism: The photooxidation of isoprene. *Atmos. Environ.* **1996**, *30*, 1255−1269.
(38) Grosjean, D.; Williams, E. L., II; Grosjean, E. Atmospheric chemistry of isoprene and of its carbonyl products. *Environ. Sci. Technol.* **1993**, *27*, 830−840.
(39) Brasseur, G. P.; Hauglustaine, D. A.; Walters, S.; Rasch, P. J.; Müller, J.-F.; Granier, C.; Tie, X. X. MOZART, a global chemical transport model for ozone and related chemical tracers, 1, Model description. *J. Geophys. Res.* **1998**, *103*, 28265−28290.
(40) Grosjean, D. Atmospheric chemistry of biogenic hydrocarbons—Relevance to the Amazon. *Quim. Nova* **1995**, *18*, 184−201.
(41) Helmig, D.; Balsley, B.; Davis, K.; Kuck, L. R.; Jensen, M.; Bognar, J.; Smith, T. Jr., Arrieta, R. V.; Rodríguez, R.; Birks, J. W. Vertical profiling and determination of landscape fluxes of biogenic nonmethane hydrocarbons within the planetary boundary layer in the Peruvian Amazon. *J. Geophys. Res.* **1998**, *103*, 25519−25532 and references therein.
(42) Geiger, H.; Barnes, I.; Bejan, I.; Benter, T.; Spittler, M. The tropospheric degradation of isoprene: an updated module for the regional atmospheric chemistry mechanism. *Atmos. Environ.* **2003**, *37*, 1503−1519.
(43) Limbeck, A.; Puxbaum, H.; Otter, L.; Scholes, M. C. Semivolatile behavior of dicarboxylic acids and other polar organic species at a rural background site (Nylsvley, RSA). *Atmos. Environ.* **2001**, *35*, 1853−1862.
(44) Baboukas, E. D.; Kanakidou, M.; Mihalopoulos, N. Carboxylic acids in gas and particulate phase above the Atlantic Ocean. *J. Geophys. Res.* **2000**, *105*, 14459−14471.
(45) Grosjean, D. Atmospheric reactions of pyruvic acid. *Atmos. Environ.* **1983**, *17*, 2379−2382.
(46) Kalberer, M.; Paulsen, D.; Sax, M.; Steinbacher, M.; Dommen, J.; Prevot, A. S. H.; Fisseha, R.; Weingartner, E.; Frankevich, V.; Zenobi, R.; Baltensperger, U. Identification of polymers as major components of atmospheric organic aerosols. *Science* **2004**, *303*, 1659−1662.
(47) Colominas, C.; Teixido, J.; Cemeli, J.; Luque, F. J.; Orozco, M. Dimerization of Carboxylic Acids: Reliability of Theoretical Calculations and the Effect of Solvent. *J. Phys. Chem. B* **1998**, *102*, 2269−2276.
(48) Katchalsky, A.; Eisenberg, H.; Lifson, S. Hydrogen Bonding and Ionization of Carboxylic Acids in Aqueous Solutions. *J. Am. Chem. Soc.* **1951**, *73*, 5889−5890.

Received for review December 12, 2004. Revised manuscript received March 21, 2005. Accepted March 29, 2005.

ES048039H